STABILITY OF DENSE STELLAR CLUSTERS AGAINST RELATIVISTIC COLLAPSE. II. MAXWELLIAN DISTRIBUTION FUNCTIONS WITH DIFFERENT CUTOFF PARAMETERS

G. S. Bisnovatyi-Kogan,[1,2] M. Merafina[1,3] R. Ruffini,[1,3] and E. Vesperini[1,4]

ABSTRACT

We investigate the stability of dense stellar clusters against relativistic collapse by approximate methods described in the previous paper in this series. These methods, together with the analysis of the fractional binding energy of the system, have been applied to sequences of equilibrium models, with cutoff in the distribution function, which generalize those studied by Zeldovich & Podurets. We show the existence of extreme configurations, which are stable all the way up to infinite values of the central redshift.

Subject headings: celestial mechanics, stellar dynamics — globular clusters: general — relativity

1. INTRODUCTION

The motivation for analyzing relativistic clusters as a way of explaining the quasar redshift as a pure gravitational redshift phenomenon (Hoyle & Fowler 1967) has been superseded by the very clear evidence of the cosmological nature of the redshift associated with the Hubble flow. On the other hand, the formation of massive black holes in active galactic nuclei (AGNs) could be the result of a collapse of dense stellar cluster (see, e.g., Rees 1984). The theoretical issue of the stability of such relativistic clusters, started by Einstein himself (1939) and continued by Zeldovich & Podurets (1965; hereafter ZP) and Zapolsky (1968), is still open.

A particular case of stable equilibrium configurations in a relativistic cluster with infinite central gravitational redshift was obtained by Bisnovatyi-Kogan & Zeldovich (1969).

In this paper we address the investigation of the stability against relativistic collapse of isothermal models generalizing those studied by ZP, setting the critical values for the onset of instability and showing also the existence of an entire two-parameter family of stable nonsingular models with arbitrarily large central redshifts (for a short version see also Merafina et al. 1996).

We consider spherically symmetric stellar clusters, with no angular momentum, described by Schwarzschild metric,

$$ds^2 = e^\nu c^2 \, dt^2 - e^\lambda \, dr^2 - r^2(d\theta^2 + \sin^2 \theta \, d\phi^2) \,, \tag{1}$$

with a distribution function given by

$$\begin{cases} f = Be^{-E/T} & \text{for } E \leq E_{\text{cut}} \equiv mc^2 - \alpha T/2 \,, \\ f = 0 & \text{for } E > E_{\text{cut}} \,, \end{cases} \tag{2}$$

where $E = e^{\nu/2}(p^2 c^2 + m^2 c^4)^{1/2}$ is the total energy of the particle star and T, in energy units, is the temperature "measured by an infinitely remote observer," constant over the cluster in equilibrium; T_r, characterizing the average kinetic energy of the stars, is $T_r = Te^{-\nu/2}$ and varies along the cluster.

The investigation of equilibrium of models with $\alpha = 1$ was considered by ZP in 1965, while the extension to models with $\alpha \neq 1$ has been previously considered by Ipser (1969) and Suffern & Fackerell (1976; hereafter SF) and then systematically analyzed by Merafina & Ruffini (1990).

In a previous paper (Bisnovatyi-Kogan et al. 1993; hereafter BMRV) we considered the issue of the stability of such configurations by analyzing the specific case of the distribution function of equation (2) with $\alpha = 1$, introduced by ZP.

In this paper we generalize the analysis of the stability of models with $\alpha \neq 1$. Spanning the entire range of possible values of α we obtain equilibrium configurations characterized by extreme core-halo density profiles and also more homogeneous configurations.

In BMRV we have formulated three criteria for the stability of clusters against relativistic collapse, based on the static approach of Zeldovich (1963) with the construction of sequences of appropriate equilibrium configurations:

1. Sequences of models with fixed cutoff parameter;
2. Sequences of models with constant specific entropy;
3. Sequences of non-Maxwellian models, constructed from the condition of conservation of adiabatic invariant, $p_{\text{cut}} \sim n^{1/3}$.

These criteria were applied, in BMRV, to the models with $\alpha = 1$, and the relationship between our criteria and those existing in literature was also examined; in particular, a close relation was shown to exist between our criterion (1) and that introduced in Ipser (1980).

In the present paper, we extend the above three criteria to the stability analysis of models with values of the parameter $\alpha \neq 1$. There is, a priori, no reason to select a specific value of α. In a certain sense, fixing a value of α corresponds to arbitrarily reducing the space of all possible models of equilibrium.

The difficulty of formulating exact criteria of dynamical stability, unlike the case of stars, arises from the fact that, in this case of collisionless clusters, correct sequences fulfilling the adiabaticity requirement cannot be rigorously constructed by writing analytically the distribution functions.

As explained in detail in BMRV, the criteria we have introduced are based on sequences along which the adiabaticity requirement is fulfilled but the Maxwellian form of the distribution function remains unchanged (criteria [1], [2]), or sequences where the deviations from the Maxwellian form are taken into account but the adiabaticity requirement is only approximately fulfilled (criterion [3]).

Nevertheless, these approximations are clearly not too severe, and the criteria are expected to supply reliable results on the critical parameters for the onset of dynamical instability. This expectation is indeed confirmed by our results: in the region with $T > 0.1 \ mc^2$ for models with $\alpha \leq 1.5$, which was already examined in previous investigations (Ipser 1969; SF), we find results in agreement with these treatments.

In § 2 we show the main properties of the equilibrium configurations in the range of small central redshifts and sufficiently large temperatures. In § 3 we briefly describe the three stability criteria introduced in BMRV and the results of the stability analysis of equilibria shown in § 2. In §§ 4 and 5 we address the equilibrium properties and the stability of the limiting solutions with $\alpha \to 0$ and those with $T \to 0$, respectively; we show the existence of stable configurations with $z_c \to \infty$. In § 6, following Merafina & Ruffini (1995), we compare the properties of a particular family of configurations with numerical models existing in literature. Finally, in § 7 we summarize the conclusions of the paper.

2. EQUILIBRIUM CONFIGURATIONS

The general relativistic equilibrium equations (Tolman 1939) for a perfect fluid of pressure P_0 and energy density ϵ_0 can be written in dimensionless form as

$$\begin{cases} e^{-\lambda_0}\left(\dfrac{1}{\tilde{r}_0}\dfrac{dv_0}{d\tilde{r}_0} + \dfrac{1}{\tilde{r}_0^2}\right) - \dfrac{1}{\tilde{r}_0^2} = 8\pi\tilde{P}_0 \ , \\[2mm] e^{-\lambda_0}\left(\dfrac{1}{\tilde{r}_0}\dfrac{d\lambda_0}{d\tilde{r}_0} - \dfrac{1}{\tilde{r}_0^2}\right) + \dfrac{1}{\tilde{r}_0^2} = 8\pi\tilde{\epsilon}_0 \ , \end{cases} \tag{3}$$

where the subscript 0 indicates unperturbed configurations with Maxwellian distribution function of equation (2). The values without this subscript are related to non-Maxwellian distributions used in criterion (3) of BMRV.

We solve here these equations for sequences of models with the distribution function given in equation (2) for different values of the parameter α. Along each sequence α is constant and T varies. The total star energy E and the momentum p are connected as

$$E = e^{v/2}(p^2 c^2 + m^2 c^4)^{1/2} \ . \tag{4}$$

The dimensional expressions of the energy density $\epsilon_0 \equiv \rho_0 c^2$, the pressure P_0, and the number density n_0 in Maxwellian case are written in the form

$$\epsilon_0 = \frac{4\pi}{c^3} B_0 e^{-3v_0/2} \int_{mc^2 e^{v_0/2}}^{mc^2 - \alpha T/2} e^{-E_0/T}\sqrt{e^{v_0}E_0^2 - m^2 c^4} \ E_0^2 \ dE_0 \ , \tag{5}$$

$$P_0 = \frac{4\pi}{3c^3} B_0 e^{-v_0/2} \int_{mc^2 e^{v_0/2}}^{mc^2 - \alpha T/2} e^{-E_0/T}(e^{-v_0}E_0^2 - m^2 c^4)^{3/2} \ dE_0 \ , \tag{6}$$

$$n_0 = \frac{4\pi}{c^3} B_0 e^{-v_0} \int_{mc^2 e^{v_0/2}}^{mc^2 - \alpha T/2} e^{-E_0/T}\sqrt{e^{-v_0}E_0^2 - m^2 c^4} \ E_0 \ dE_0 \ . \tag{7}$$

The dimensionless variables used for the numerical solution are

$$\tilde{T} = \frac{T}{mc^2} \ , \qquad x_0 = \frac{E_0}{mc^2} \ , \qquad \tilde{r}_0 = \frac{r_0}{r_{0*}} \ , \qquad \tilde{n}_0 = \frac{n_0}{n_{0*}} \ , \qquad \tilde{P}_0 = \frac{P_0}{P_{0*}} \ , \qquad \tilde{\epsilon}_0 = \frac{\epsilon_0}{\epsilon_{0*}} \ , \tag{8}$$

where

$$n_{0*} = \frac{4\pi}{c^3} B_0 (mc^2)^3 \ , \qquad P_{0*} = \epsilon_{0*} = \frac{4\pi}{c^3} B_0 (mc^2)^4 \ , \qquad r_{0*} = (m^2 \sqrt{4\pi GcB_0})^{-1} \ . \tag{9}$$

The corresponding dimensionless expression for energy density, pressure, and number density are written, respectively, as

$$\tilde{\epsilon}_0 = e^{-3v_0/2} \int_{e^{v_0/2}}^{1 - \alpha\tilde{T}/2} e^{-x_0/\tilde{T}}\sqrt{e^{-v_0}x_0^2 - 1} \ x_0^2 \ dx_0 \ , \tag{10}$$

$$\tilde{P}_0 = \tfrac{1}{3}e^{-v_0/2} \int_{e^{v_0/2}}^{1 - \alpha\tilde{T}/2} e^{-x_0/\tilde{T}}(e^{-v_0}x_0^2 - 1)^{3/2} \ dx_0 \ , \tag{11}$$

$$\tilde{n}_0 = e^{-v_0} \int_{e^{v_0/2}}^{1 - \alpha \tilde{T}/2} e^{-x_0/\tilde{T}} \sqrt{e^{-v_0} x_0^2 - 1} \, x_0 \, dx_0 \ . \tag{12}$$

At a given $\tilde{T}$ and α, the solution of the equation (3) is determined uniquely by the boundary conditions

$$\lambda_0(0) = 0 \ , \qquad v_0(0) = v_{c0} \ , \tag{13}$$

where $v_{c0}(\tilde{T}, \alpha)$ is calculated by the condition at boundary $\tilde{r}_0 = \tilde{R}_0$, where $e^{v_0(\tilde{R}_0)/2} = 1 - \alpha \tilde{T}/2 = (1 - 2\tilde{M}_0/\tilde{R}_0)^{1/2}$ and the solution smoothly matches the Schwarzschild solution,

$$v_0(\tilde{R}_0) + \lambda_0(\tilde{R}_0) = 0 \ . \tag{14}$$

The dimensionless mass $\mathscr{M}_0(\tilde{r}_0)$ within a given radius $\tilde{r}_0$ and the total number of stars of the cluster $\tilde{N}_0$, proportional to its rest mass, are given by the formulae

$$\mathscr{M}_0(\tilde{r}_0) = \int_0^{\tilde{r}_0} 4\pi \tilde{\epsilon}_0 \, \tilde{r}_0'^2 \, d\tilde{r}_0' \ , \qquad \text{with } \tilde{M}_0 = \mathscr{M}_0(\tilde{R}_0) \ , \tag{15}$$

and

$$\tilde{N}_0 = \int_0^{\tilde{R}_0} 4\pi \tilde{n}_0 \, e^{\lambda_0/2} \tilde{r}_0'^2 \, d\tilde{r}_0' \ , \tag{16}$$

where $e^{\lambda_0} = [1 - 2\mathscr{M}_0(\tilde{r}_0)/\tilde{r}_0]^{-1}$, $\tilde{\mathscr{M}}_0(\tilde{r}_0) = \mathscr{M}_0(r_0)/(\epsilon_{0*} r_{0*}^3 c^2)$, and $\tilde{N}_0 = N_0/(n_{0*} r_{0*}^3)$.

The results of integrations are given in Figures 1–2, where the main dimensionless parameters for the models are presented. It is interesting to note from Figure 1 that the maximum mass of the sequences of the equilibrium configurations tends to a limiting value, for $\alpha \to 0$. Moreover, for sequences with $\alpha > 1.5$ different branches of the same family of solutions at fixed α appear (see, e.g., $\alpha = 2.0$). This particular feature is also evident in Figure 2 where the central redshift, $z_c = e^{v_0/2} - 1$, of the sequences of equilibrium models at fixed α is given as a function of the temperature. At small $\tilde{T}$, the curves deform, and they split in more parts: one or more loops and one curve all coming out from the origin.

The calculations have shown that equilibrium solutions exist only for $\alpha < \alpha_{\text{lim}}(\tilde{T})$. This limit is decreasing with increasing temperature and tends to zero at very large temperature (see Fig. 3). Thus, only configurations with $\alpha \to 0$ exist for very large values of the temperature, corresponding to the limiting solution described in § 4.

The Newtonian limit corresponds to $\tilde{T} \to 0$ and can be investigated separately using equations (7)–(9) of BMRV. For this case a unique curve $\tilde{M}(\alpha)$ or $\tilde{M}(\rho_c)$ can be plotted (Figs. 4a–4b) showing that $\alpha \to 2.02$ for $\rho_c \to \infty$. It is evident also in Figure 4a the particular behavior of the solutions with $\alpha > 1.5$: there are more solutions with different values of the mass at the same
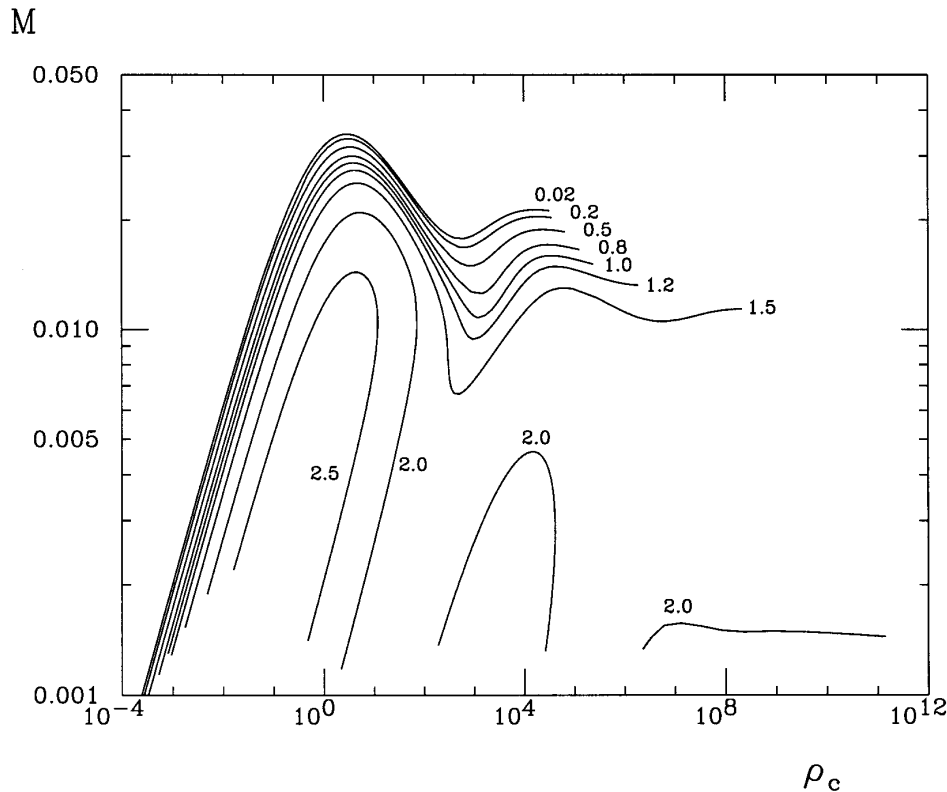

FIG. 1.—Mass of the equilibrium configurations as a function of the central density along sequences at fixed value of α (labeled on the curves). Quantities are given in arbitrary units.
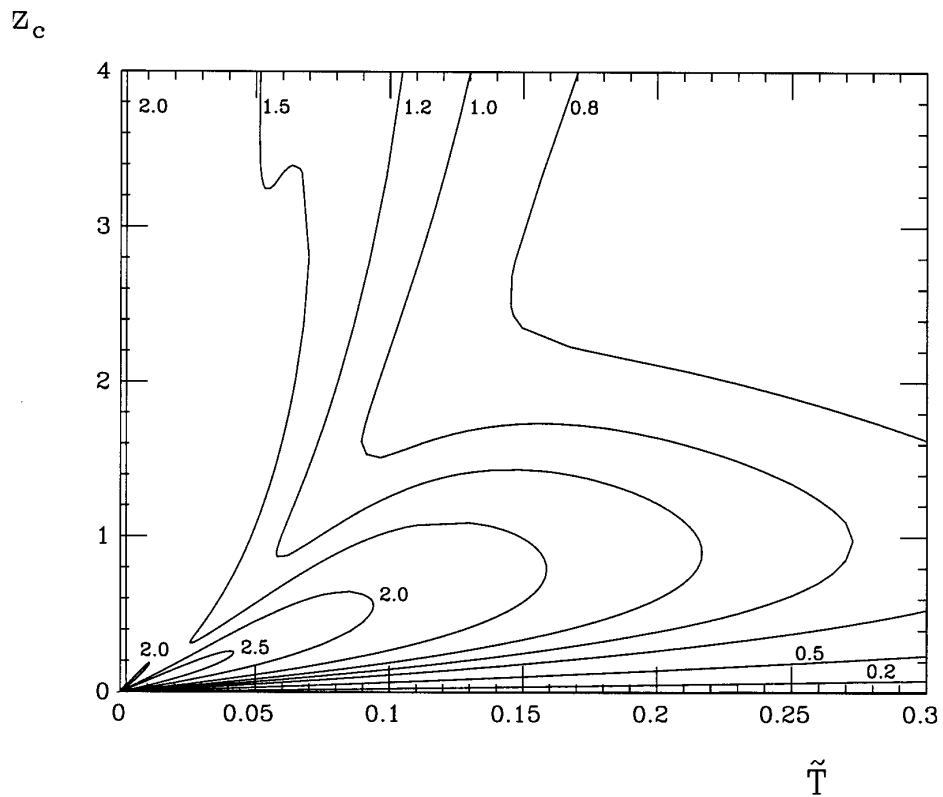
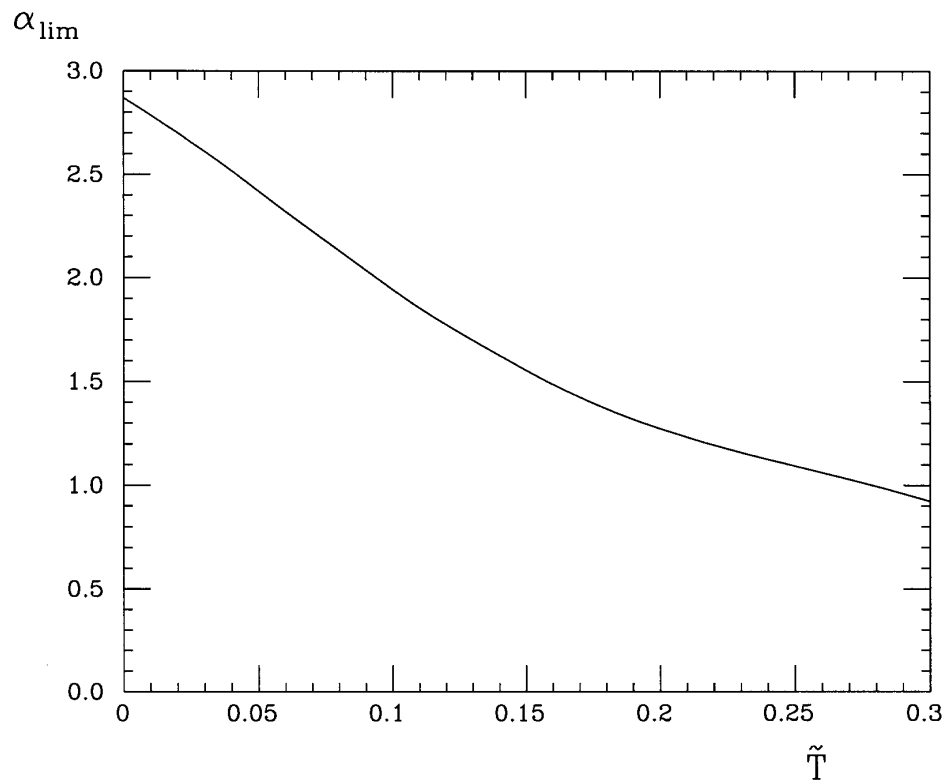FIG. 2.—Sequences with different values of α in the plane z_c-$\tilde{T}$

FIG. 3.—Limiting value of α as a function of the temperature $\tilde{T}$. The absolute maximum value is reached at $\tilde{T} \to 0$ and corresponds to $\alpha_M = 2.87$.
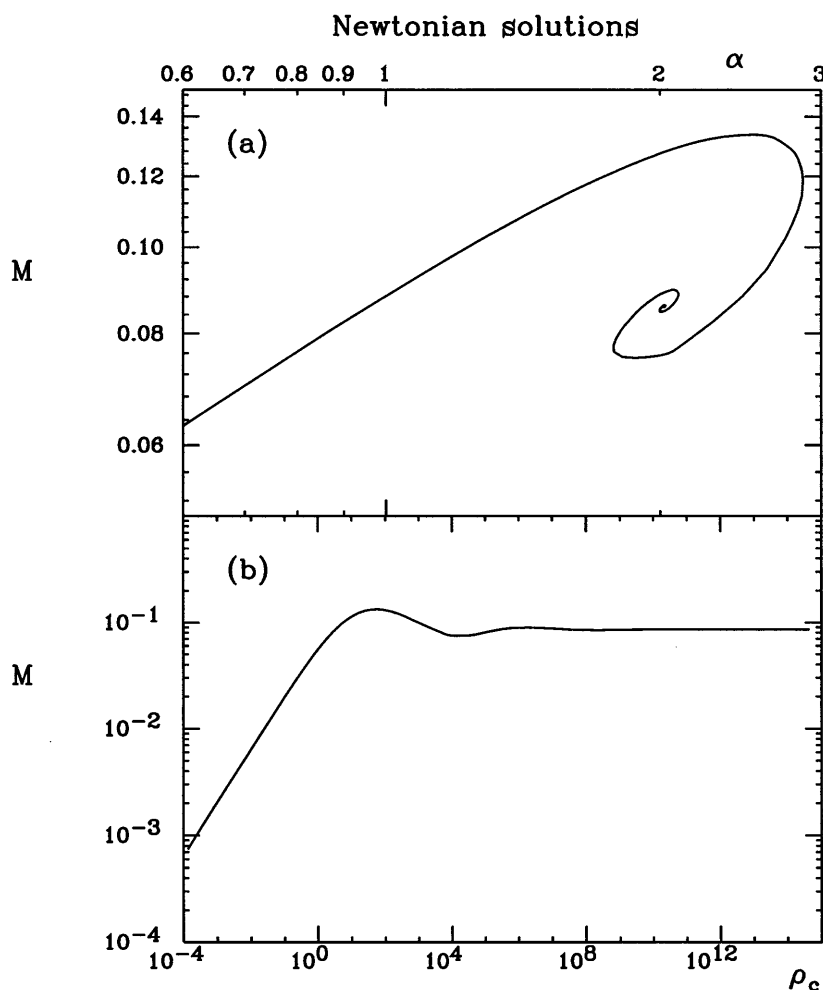
Newtonian solutions

Fig. 4.—(a) Mass of the Newtonian solutions as a function of the parameter α. The limiting value of α (*center of the spiral*), corresponding to an infinite value of the central density, is equal to 2.02. (b) Mass of the Newtonian solutions as a function of the central density. Mass and density are given in arbitrary units.

value of the parameter α. The maximum value of α for a Newtonian solution corresponds to the maximum value of any relativistic solution, easily deducible also from Figure 3 for $\tilde{T} \to 0$: *there are no solutions with α larger than $\alpha_M = 2.87$*. These models, obtained in the framework of the Newtonian formalism, can also reach very large values of central gravitational potential ($\psi_0 \to +\infty$) and central density ($\rho_c \to +\infty$).

The GR family of the equilibrium curves $M_{\tilde{T}}(\alpha)$ or $M_{\tilde{T}}(\rho_c)$, are plotted in the Figures 5a–5b. It is interesting to note two kinds of oscillations existing in the curves $M_\alpha(\rho_c)$ (Fig. 1) and $M_{\tilde{T}}(\rho_c)$ (Fig. 5b). The oscillations in the curve $M_\alpha(\rho_c)$ for $\alpha \leq 1.5$ have pure relativistic origin (see, e.g., Harrison et al. 1965); they are connected with the stability analysis and correspond to an increase of unstable modes for increasing values of ρ_c. The second class of oscillations is evident in the curve $M_{\tilde{T}}(\rho_c)$; it has no relation with stability but reflects oscillatory properties of an isothermal configuration, not yet clearly understandable, similar to the density oscillations in the equilibrium curve $\rho(r)$ (see, e.g., Chandrasekhar 1939).

Further, it is important to note that while in neutron stars and white dwarfs, because of the uniqueness of the equation of state of matter in the ground state, the onset of gravitational instability occurs at a unique value of central gravitational redshift and at a specific value of the mass, called the *critical mass against gravitational collapse*, in the present case of relativistic clusters the equation of state, defined by equations (10)–(12), is a function of the temperature and the cutoff parameter. Consequently, the region of stability and the onset of gravitational instability are defined *not* by a unique value of the critical mass but by a *continuous line* in the z_c-$\tilde{T}$ plane (see § 5).

Finally, for completeness, we would like to recall here the discussion of some features on the structures of the equilibrium configurations pointing to a novel classification of stable relativistic clusters recently analyzed by Merafina & Ruffini (1997). In this classification attention is given to the region S2 (see Figure 9 below): the novelty is that these configurations, unlike those of the region S1, do present a double feature of a relativistic core and an extended halo.

The general relativistic models for small values of $\tilde{T}$ have small values of the ratio $2GM/Rc^2$, ranging from Newtonian regimes, where $2GM/Rc^2 \ll 1$, all the way to a mildly relativistic regime with $2GM/Rc^2 \sim 0.09$, for $\tilde{T} \simeq 0.06$. Moreover, they have very large values of z_c in the limit of large values of the central density ρ_c. In this regime the equilibrium configurations present a regular center without singularities even for arbitrarily large central densities. However, they have extreme core-halo structures, the core being up to only 10^{-4} times the radius of the cluster.
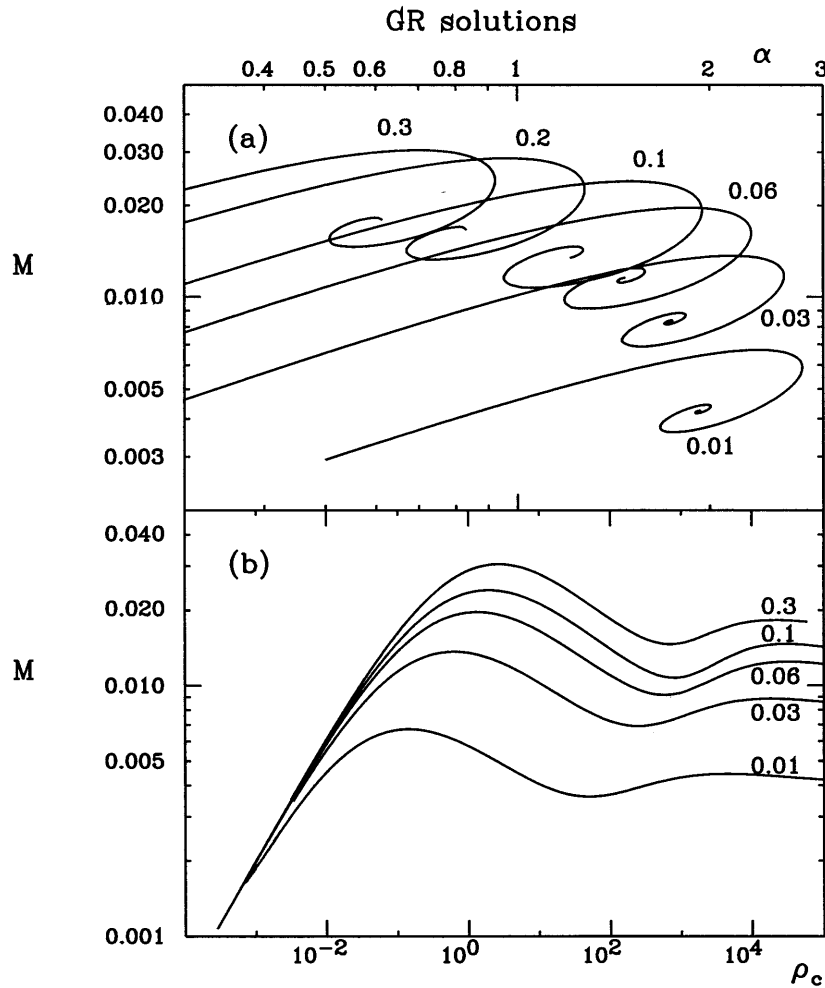
GR solutions

FIG. 5.—(a) Mass of the relativistic solutions as a function of the parameter α for fixed values of the temperature $\tilde{T}$ (labeled on the curves). (b) Mass of the relativistic solutions as a function of the central density for fixed values of the temperature $\tilde{T}$ (labeled on the curves). Mass and density are given in arbitrary units.

In order to illustrate the explicit density distribution and metric coefficients, two specific configurations are examined: one in the traditional family (region S1) with $z_c \lesssim 0.5$ (config. 1) studied by Ipser (1969) and one in the region S2 at low temperatures and large values of the central redshift (config. 2). These configurations are discussed in detail in Figure 6 where the metric coefficients, the density profiles, and the local circular velocities are shown. It is important to note that in configuration 1 the maximum of e^{λ} occurs very close to the radius R of the configuration, while in configuration 2 the existence of a compact core is clearly manifested by the occurrence of the maximum of e^{λ} deeply inside the configuration at $r \sim 10^{-3} R$. It is also important to emphasize the fact that the dense cores cannot exist " bare," i.e., without their extended, almost Newtonian envelopes. The global stability of the cluster appears to demand the existence of both components: the relativistic core *and* the halo.

3. STABILITY ANALYSIS

Since the sequence of the models $M(\rho_c)$ at given α is not good enough in the intermediate region for stability analysis, we use three different sequences from BMRV. In this section we investigate the stability of models with $\alpha < 1.5$, where the criteria give reliable results. First, for $\alpha \geq 1.5$, the criterion based on sequences with a fixed specific entropy gives results of difficult interpretation, which is due to a particular oscillatory behavior after the first maximum that appears in the mass-radius relation relevant to the stability analysis; second, the criterion based on sequences with the conservation of the adiabatic invariant does not apply well at these regimes because of changes from increasing to decreasing behavior of the central density in families at constant α (see Fig. 1). The only criterion that gives results with sufficient accuracy also for models with $\alpha \geq 1.5$ is that based on sequences with a fixed cutoff (see § 5), even if it is less precise than the other two in the regime $\alpha < 1.5$.

We will investigate the stability of models with $\alpha \geq 1.5$ in § 5.

3.1. *Sequences with a Fixed Cutoff Parameter*

The parameters

$$W_0 = \left(\frac{\epsilon_{cut}}{T_r}\right)_{r=0} \qquad \text{and} \qquad \beta = \frac{T_R}{mc^2} \, , \tag{17}$$

Fig. 6.—(a) Metric elements e^λ, e^ν are plotted as a function of the radial coordinate for a particular solution with $\tilde{T} = 0.09$ and $z_c = 0.13$ (co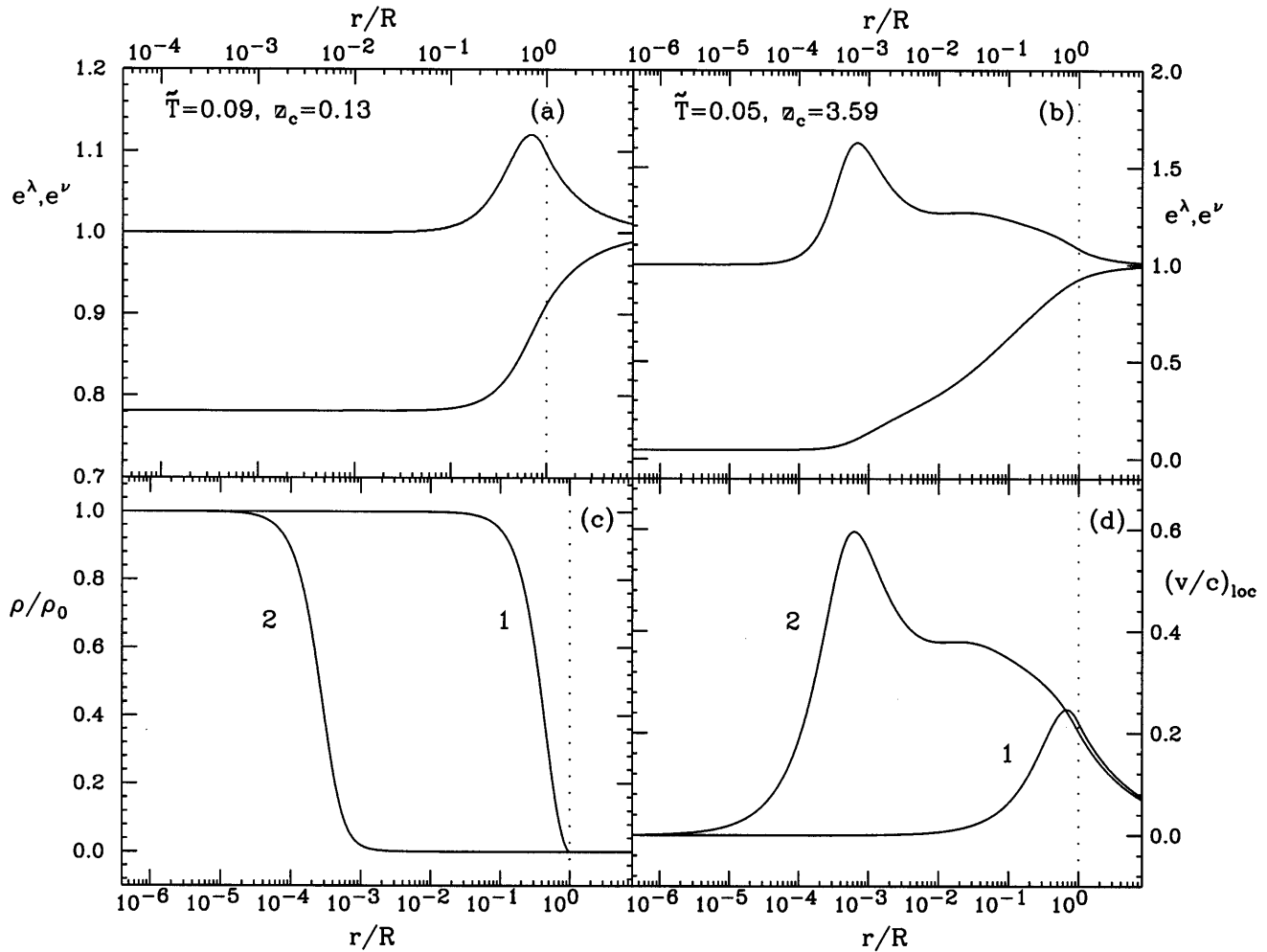nfig. 1). (b) Metric elements e^λ, e^ν are plotted as a function of the radial coordinate for a particular solution with $\tilde{T} = 0.05$ and $z_c = 3.59$ (config. 2). (c) Density profile as a function of the radial coordinate is shown for the two particular solutions. (d) Local circular velocity is given as a function of the radial coordinate for the two particular solutions.

where $T_r = Te^{-\nu/2}$ is the local temperature varying along the cluster and $\epsilon_{\rm cut} = (p_{\rm cut}^2 c^2 + m^2 c^4)^{1/2} - mc^2 = Ee^{-\nu/2} - mc^2$ is the kinetic energy cutoff, were used by Merafina & Ruffini (1989) instead of $\tilde{T} = T/mc^2$ and α of ZP. They are related by the following expressions:

$$\beta = \frac{\tilde{T}}{1 - \alpha\tilde{T}/2} \tag{18}$$

and

$$W_0 = \frac{1 - e^{\nu(0)/2}}{\tilde{T}} - \frac{\alpha}{2} . \tag{19}$$

The first of the sequences used for stability analysis is the sequence with constant W_0 and varying β. As shown in BMRV, the parameter W_0 can be taken as approximately adiabatic; sequences with α constant and varying $\tilde{T}$ correspond to sequences with β varying and W_0 changing slowly, at least until the first maximum of $\tilde{T}$, in accordance with equation (19) (see Fig. 7). The equivalence of this stability criterion with that suggested by Ipser (1980) was definitely shown in BMRV for $\alpha = 1$: this sequence near the critical point corresponds to that relevant in the application of Ipser's criterion. This correlation near the critical point is also retained at $\alpha \neq 1$ for models with $\tilde{T} > 1.5$ and leads to results in accordance with those given in literature.

Results of the application of this criterion for models with $\alpha < 1.5$ are given in Table 1.

3.2. Sequences with a Fixed Specific Entropy

We introduce the expression of the entropy of a system with arbitrary distribution function,

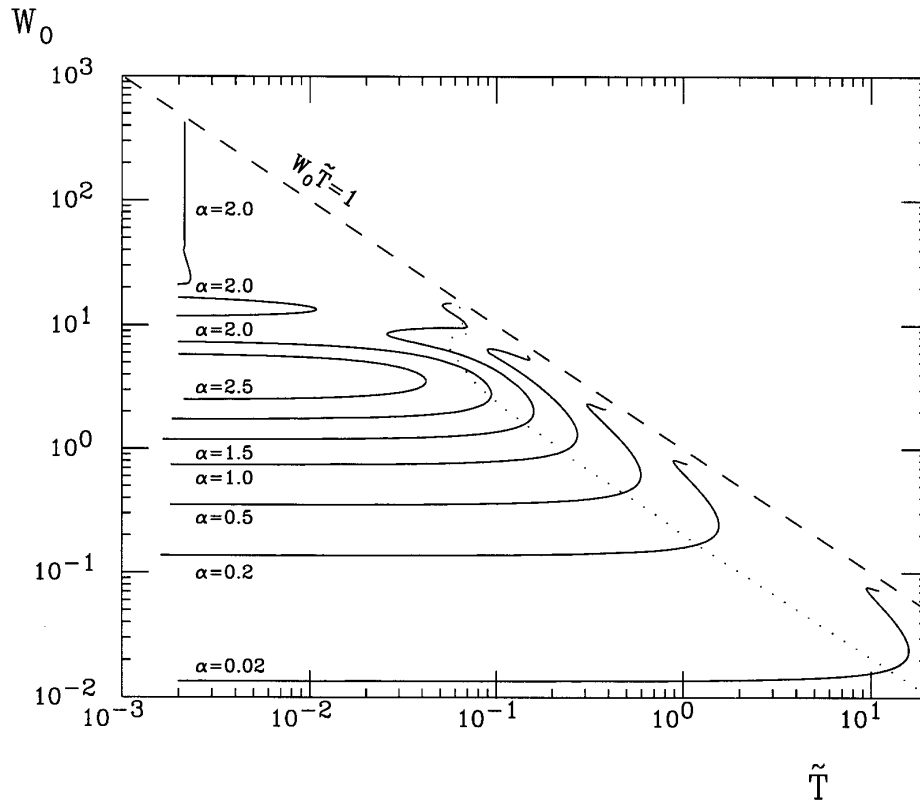$$S = \iint f(1 - \ln f) \, d^3p \, d^3r , \tag{20}$$

W$_0$

FIG. 7.—Cutoff parameter W_0 shown as a function of the temperature $\tilde{T}$, for sequences at fixed values of α (labeled on the curves). The equilibria are limited by the condition $W_0 \tilde{T} < 1$ (*dashed line*), obtainable from eqs. (18)–(19) and the definition of central redshift $z_c = e^{-v_0/2} - 1$. Dotted line indicates the onset of instability. Notice that there are no unstable models for $\tilde{T} \lesssim 0.06$.

and we investigate the sequences with the fixed specific entropy S/N_0, where N_0 is the total number of stars, whose dimensionless expression is given by equation (16). Using equations (2), (16), and (20) we can obtain for the specific entropy the expression

$$s \equiv \frac{S}{N_0} = \left[1 - \ln\left(\frac{B}{B_*}\right) \right] + \frac{\int_0^R e^{(\lambda + v)/2} \epsilon r^2 \, dr}{T \int_0^R e^{\lambda/2} n r^2 \, dr} , \tag{21}$$

where B_* is an arbitrary constant along the sequence with the dimension of B.

The sequences with fixed entropy were considered by BMRV as the second set of sequences for stability investigation. Here these sequences are used for stability investigation of models with $\alpha < 1.5$. The results are presented in Table 2.

3.3. *Sequences with Conservation of the Adiabatic Invariant*

The conservation of the adiabatic invariant $I = p n_c^{-1/3}$ (Podurets 1969) along the sequence of models implies the introduction of non-Maxwellian distribution functions

$$f = B \exp\left\{ -\frac{e^{v/2}}{T_0} \left[p^2 c^2 \left(\frac{n_{c0}}{n_c}\right)^{2/3} + m^2 c^4 \right]^{1/2} \right\}, \tag{22}$$

with the cutoff parameters

$$p_{cut} = p_{cut0} \left(\frac{n_c}{n_{c0}}\right)^{1/3} = \frac{p_{cut0}}{\kappa}, \qquad \kappa = \left(\frac{n_{c0}}{n_c}\right)^{1/3} . \tag{23}$$

The expression for p_{cut0} is determined from the cutoff relation of the initial Maxwellian model with $T = T_0$ and $v = v_0(r)$; we have

$$(p_{cut0}^2 c^2 + m^2 c^4)^{1/2} e^{v_0(r)/2} = mc^2 - \alpha T/2 . \tag{24}$$

The procedure of constructing approximate equilibrium models with a non-Maxwellian distribution function is described in detail by BMRV as well as a method of constructing the sequences of models for stability analysis. Here we use exactly the same method for models with $\alpha < 1.5$. The results are presented in Table 3.

4. THE LIMITING SOLUTION AT $\alpha \to 0$

It is interesting to investigate the limiting solution corresponding to $\alpha \to 0$, $T \to \infty$, and $\alpha T = \eta$. Since in this limit $e^{-E/T} \simeq 1$, the expressions of the most relevant quantities in the calculation of the equilibrium properties assume a more simplified form. The importance of this limiting solution lies in the fact that the properties of the equilibrium solutions with a

TABLE 1

NUMERICAL RESULTS OF STABILITY ANALYSIS BASED ON STATIC CRITERION OF SEQUENCES AT CONSTANT W_0 ($\alpha < 1.5$)

α	W_0	ρ_c	M	N	R	$\tilde{T}$	z_c
1.20......	1.190×10^0	5.305×10^0	2.73278×10^{-2}	2.834×10^{-2}	2.626×10^{-1}	1.84×10^{-1}	4.886×10^{-1}
		5.371×10^0	2.73291×10^{-2}	2.834×10^{-2}	2.619×10^{-1}	1.84×10^{-1}	4.916×10^{-1}
		5.437×10^0	2.73299×10^{-2}	2.834×10^{-2}	2.611×10^{-1}	1.84×10^{-1}	4.946×10^{-1}
1.20......	1.193×10^0	5.406×10^0	2.73137×10^{-2}	2.833×10^{-2}	2.615×10^{-1}	1.85×10^{-1}	4.929×10^{-1}
		5.473×10^0	2.73143×10^{-2}	2.833×10^{-2}	2.607×10^{-1}	1.85×10^{-1}	4.959×10^{-1}
		5.540×10^0	2.73142×10^{-2}	2.833×10^{-2}	2.600×10^{-1}	1.85×10^{-1}	4.989×10^{-1}
1.20......	1.197×10^0	5.513×10^0	2.72934×10^{-2}	2.830×10^{-2}	2.603×10^{-1}	1.86×10^{-1}	4.972×10^{-1}
		5.581×10^0	2.72932×10^{-2}	2.830×10^{-2}	2.595×10^{-1}	1.86×10^{-1}	5.003×10^{-1}
		5.650×10^0	2.72926×10^{-2}	2.830×10^{-2}	2.588×10^{-1}	1.86×10^{-1}	5.034×10^{-1}
0.50......	4.429×10^{-1}	3.542×10^0	3.17653×10^{-2}	3.294×10^{-2}	2.870×10^{-1}	4.72×10^{-1}	4.829×10^{-1}
		3.586×10^0	3.17660×10^{-2}	3.294×10^{-2}	2.861×10^{-1}	4.72×10^{-1}	4.858×10^{-1}
		3.629×10^0	3.17661×10^{-2}	3.294×10^{-2}	2.853×10^{-1}	4.72×10^{-1}	4.887×10^{-1}
0.50......	4.433×10^{-1}	3.570×10^0	3.17630×10^{-2}	3.294×10^{-2}	2.864×10^{-1}	4.73×10^{-1}	4.847×10^{-1}
		3.614×10^0	3.17634×10^{-2}	3.294×10^{-2}	2.856×10^{-1}	4.73×10^{-1}	4.877×10^{-1}
		3.658×10^0	3.17631×10^{-2}	3.294×10^{-2}	2.847×10^{-1}	4.73×10^{-1}	4.906×10^{-1}
0.50......	4.436×10^{-1}	3.598×10^0	3.17614×10^{-2}	3.294×10^{-2}	2.859×10^{-1}	4.74×10^{-1}	4.865×10^{-1}
		3.642×10^0	3.17614×10^{-2}	3.294×10^{-2}	2.851×10^{-1}	4.74×10^{-1}	4.895×10^{-1}
		3.687×10^0	3.17608×10^{-2}	3.294×10^{-2}	2.842×10^{-1}	4.74×10^{-1}	4.925×10^{-1}
0.20......	1.704×10^{-1}	3.008×10^0	3.34394×10^{-2}	3.468×10^{-2}	2.984×10^{-1}	1.20×10^0	4.744×10^{-1}
		3.082×10^0	3.34426×10^{-2}	3.468×10^{-2}	2.966×10^{-1}	1.20×10^0	4.801×10^{-1}
		3.157×10^0	3.34433×10^{-2}	3.468×10^{-2}	2.949×10^{-1}	1.20×10^0	4.859×10^{-1}
0.20......	1.709×10^{-1}	3.068×10^0	3.34386×10^{-2}	3.468×10^{-2}	2.969×10^{-1}	1.21×10^0	4.790×10^{-1}
		3.144×10^0	3.34397×10^{-2}	3.468×10^{-2}	2.952×10^{-1}	1.21×10^0	4.848×10^{-1}
		3.221×10^0	3.34384×10^{-2}	3.468×10^{-2}	2.934×10^{-1}	1.21×10^0	4.907×10^{-1}
0.20......	1.716×10^{-1}	3.182×10^0	3.34354×10^{-2}	3.468×10^{-2}	2.943×10^{-1}	1.22×10^0	4.877×10^{-1}
		3.261×10^0	3.34329×10^{-2}	3.467×10^{-2}	2.926×10^{-1}	1.22×10^0	4.937×10^{-1}
		3.342×10^0	3.34278×10^{-2}	3.467×10^{-2}	2.908×10^{-1}	1.22×10^0	4.996×10^{-1}
0.02......	1.669×10^{-2}	2.760×10^0	3.43941×10^{-2}	3.567×10^{-2}	3.047×10^{-1}	1.21×10^1	4.706×10^{-1}
		2.828×10^0	3.43984×10^{-2}	3.568×10^{-2}	3.029×10^{-1}	1.21×10^1	4.763×10^{-1}
		2.896×10^0	3.44001×10^{-2}	3.568×10^{-2}	3.011×10^{-1}	1.21×10^1	4.820×10^{-1}
0.02......	1.674×10^{-2}	2.847×10^0	3.43988×10^{-2}	3.568×10^{-2}	3.024×10^{-1}	1.22×10^1	4.779×10^{-1}
		2.917×10^0	3.43997×10^{-2}	3.568×10^{-2}	3.006×10^{-1}	1.22×10^1	4.836×10^{-1}
		2.988×10^0	3.43982×10^{-2}	3.568×10^{-2}	2.989×10^{-1}	1.22×10^1	4.894×10^{-1}
0.02......	1.682×10^{-2}	2.938×10^0	3.43991×10^{-2}	3.568×10^{-2}	3.001×10^{-1}	1.23×10^1	4.854×10^{-1}
		3.011×10^0	3.43967×10^{-2}	3.567×10^{-2}	2.983×10^{-1}	1.23×10^1	4.912×10^{-1}
		3.085×10^0	3.43918×10^{-2}	3.567×10^{-2}	2.965×10^{-1}	1.23×10^1	4.972×10^{-1}

NOTE.—The second configuration of each group belongs to the equilibrium sequence. For each value of α, the configuration coinciding with the maximum mass in the sequence at constant W_0 corresponds to the critical one.

sufficiently small value of α and large value of T converge to it. This behavior is clearly shown in Figure 1 where the solutions asymptotically converge to a limiting sequence for $\alpha \to 0$.

Thus, number density n_0, energy density ϵ_0, and pressure P_0 depend only on the parameter η, and the explicit dependence on the temperature T and the cutoff parameter α disappears:

$$n_0 = \frac{4\pi}{c^3} B_0 e^{-v_0} \int_{mc^2 e^{v0/2}}^{mc^2 - \eta/2} \sqrt{e^{-v_0}E_0^2 - m^2c^4} E_0 \, dE_0 \ , \tag{25}$$

$$\epsilon_0 = \frac{4\pi}{c^3} B_0 e^{-3v_0/2} \int_{mc^2 e^{v0/2}}^{mc^2 - \eta/2} \sqrt{e^{-v_0}E_0^2 - m^2c^4} E_0^2 \, dE_0 \ , \tag{26}$$

$$P_0 = \frac{4\pi}{3c^3} B_0 e^{-v_0/2} \int_{mc^2 e^{v0/2}}^{mc^2 - \eta/2} (e^{-v_0}E_0^2 - m^2c^4)^{3/2} \, dE_0 \ . \tag{27}$$

The stability of this limiting solution has been investigated by the method of conservation of adiabatic invariant, introduced in § 3.3. The parameter $\eta = \alpha T$ does not change during the perturbation, so the perturbed quantities keep the simple form:

$$n = \frac{4\pi}{c^3 \kappa^3} B e^{-v} \int_{mc^2 e^{v/2}}^{(mc^2 - \eta/2)e^{(v-v0)/2}} \sqrt{e^{-v}E^2 - m^2c^4} E \, dE \ , \tag{28}$$

$$\epsilon = \frac{4\pi}{c^3 \kappa^4} B e^{-v} \int_{mc^2 e^{v/2}}^{(mc^2 - \eta/2)e^{(v-v0)/2}} \sqrt{(E^2 e^{-v} - m^2c^4 + m^2c^4\kappa^2)(e^{-v}E^2 - m^2c^4)} E \, dE \ , \tag{29}$$

$$P = \frac{4\pi}{3c^3 \kappa^4} B e^{-v} \int_{mc^2 e^{v/2}}^{(mc^2 - \eta/2)e^{(v-v0)/2}} (E^2 e^{-v} - m^2c^4 + m^2c^4\kappa^2)^{-1/2}(e^{-v}E^2 - m^2c^4)^{3/2} E \, dE \ , \tag{30}$$

where κ was defined in equation (23).

TABLE 2

NUMERICAL RESULTS OF STABILITY ANALYSIS BASED ON STATIC CRITERION OF SEQUENCES AT CONSTANT ENTROPY ($\alpha < 1.5$)

α	S/N	ρ_c	M	N	R	$\tilde{T}$	z_c
1.20......	5.691×10^0	4.733×10^0	2.7409×10^{-2}	2.842×10^{-2}	2.697×10^{-1}	1.79×10^{-1}	4.640×10^{-1}
		4.773×10^0	2.7410×10^{-2}	2.842×10^{-2}	2.692×10^{-1}	1.79×10^{-1}	4.659×10^{-1}
		4.813×10^0	2.7411×10^{-2}	2.842×10^{-2}	2.687×10^{-1}	1.80×10^{-1}	4.678×10^{-1}
1.20......	5.640×10^0	4.924×10^0	2.7388×10^{-2}	2.840×10^{-2}	2.672×10^{-1}	1.81×10^{-1}	4.724×10^{-1}
		4.966×10^0	2.7388×10^{-2}	2.840×10^{-2}	2.667×10^{-1}	1.81×10^{-1}	4.744×10^{-1}
		5.008×10^0	2.7388×10^{-2}	2.840×10^{-2}	2.662×10^{-1}	1.81×10^{-1}	4.763×10^{-1}
1.20......	5.615×10^0	5.022×10^0	2.7377×10^{-2}	2.839×10^{-2}	2.660×10^{-1}	1.81×10^{-1}	4.767×10^{-1}
		5.065×10^0	2.7376×10^{-2}	2.839×10^{-2}	2.655×10^{-1}	1.82×10^{-1}	4.787×10^{-1}
		5.109×10^0	2.7375×10^{-2}	2.839×10^{-2}	2.650×10^{-1}	1.82×10^{-1}	4.807×10^{-1}
0.50......	2.792×10^0	3.381×10^0	3.1772×10^{-2}	3.295×10^{-2}	2.902×10^{-1}	4.65×10^{-1}	4.719×10^{-1}
		3.447×10^0	3.1774×10^{-2}	3.295×10^{-2}	2.889×10^{-1}	4.67×10^{-1}	4.764×10^{-1}
		3.515×10^0	3.1774×10^{-2}	3.295×10^{-2}	2.876×10^{-1}	4.70×10^{-1}	4.810×10^{-1}
0.50......	2.788×10^0	3.407×10^0	3.1773×10^{-2}	3.295×10^{-2}	2.896×10^{-1}	4.66×10^{-1}	4.738×10^{-1}
		3.474×10^0	3.1774×10^{-2}	3.295×10^{-2}	2.883×10^{-1}	4.68×10^{-1}	4.784×10^{-1}
		3.543×10^0	3.1773×10^{-2}	3.295×10^{-2}	2.870×10^{-1}	4.71×10^{-1}	4.830×10^{-1}
0.50......	2.783×10^0	3.434×10^0	3.1772×10^{-2}	3.295×10^{-2}	2.892×10^{-1}	4.67×10^{-1}	4.756×10^{-1}
		3.502×10^0	3.1772×10^{-2}	3.295×10^{-2}	2.878×10^{-1}	4.69×10^{-1}	4.802×10^{-1}
		3.572×10^0	3.1771×10^{-2}	3.295×10^{-2}	2.864×10^{-1}	4.71×10^{-1}	4.849×10^{-1}
0.20......	1.701×10^0	2.857×10^0	3.3433×10^{-2}	3.467×10^{-2}	3.021×10^{-1}	1.18×10^0	4.672×10^{-1}
		2.968×10^0	3.3441×10^{-2}	3.468×10^{-2}	2.993×10^{-1}	1.19×10^0	4.761×10^{-1}
		3.084×10^0	3.3442×10^{-2}	3.468×10^{-2}	2.965×10^{-1}	1.21×10^0	4.852×10^{-1}
0.20......	1.697×10^0	2.910×10^0	3.3439×10^{-2}	3.468×10^{-2}	3.008×10^{-1}	1.19×10^0	4.716×10^{-1}
		3.024×10^0	3.3443×10^{-2}	3.468×10^{-2}	2.980×10^{-1}	1.20×10^0	4.806×10^{-1}
		3.143×10^0	3.3440×10^{-2}	3.468×10^{-2}	2.952×10^{-1}	1.21×10^0	4.899×10^{-1}
0.20......	1.693×10^0	2.965×10^0	3.3442×10^{-2}	3.468×10^{-2}	2.994×10^{-1}	1.19×10^0	4.753×10^{-1}
		3.082×10^0	3.3442×10^{-1}	3.468×10^{-2}	2.966×10^{-1}	1.21×10^0	4.845×10^{-1}
		3.205×10^0	3.3436×10^{-2}	3.467×10^{-2}	2.938×10^{-1}	1.22×10^0	4.938×10^{-1}
0.02......	1.069×10^0	2.681×10^0	3.4389×10^{-2}	3.566×10^{-2}	3.069×10^{-1}	1.20×10^1	4.677×10^{-1}
		2.784×10^0	3.4396×10^{-2}	3.567×10^{-2}	3.041×10^{-1}	1.21×10^1	4.765×10^{-1}
		2.892×10^0	3.4397×10^{-2}	3.567×10^{-2}	3.013×10^{-1}	1.22×10^1	4.856×10^{-1}
0.02......	1.068×10^0	2.764×10^0	3.4398×10^{-2}	3.568×10^{-2}	3.046×10^{-1}	1.21×10^1	4.749×10^{-1}
		2.872×10^0	3.4400×10^{-2}	3.568×10^{-2}	3.018×10^{-1}	1.22×10^1	4.840×10^{-1}
		2.985×10^0	3.4396×10^{-2}	3.568×10^{-2}	2.990×10^{-1}	1.23×10^1	4.933×10^{-1}
0.02......	1.068×10^0	2.852×10^0	3.4401×10^{-2}	3.568×10^{-2}	3.022×10^{-1}	1.22×10^1	4.815×10^{-1}
		2.965×10^0	3.4399×10^{-2}	3.568×10^{-2}	2.994×10^{-1}	1.23×10^1	4.908×10^{-1}
		3.084×10^0	3.4389×10^{-2}	3.567×10^{-2}	2.965×10^{-1}	1.24×10^1	5.004×10^{-1}

NOTE.—The second configuration of each group belongs to the equilibrium sequence. For each value of α, the configuration coinciding with the maximum mass in the sequence at constant entropy corresponds to the critical one.

The instability sets in at $(\eta/mc^2)_{\rm crit} = 0.2439$, corresponding to a central redshift $z_c = 0.4832$. It is interesting to note that the critical value of $\tilde{T}$ is increasing with decreasing values of α; a similar behavior of the critical value of $\tilde{T}$ was found by Ipser (1969) for some values of α. The value of the quantity $(\alpha\tilde{T})_{\rm cr}$ increases with decreasing values of α also and tends to a constant value $(\alpha\tilde{T})_{\rm cr} = 0.2239$. Given the relation between $\alpha\tilde{T}$ and the cutoff energy $E_{\rm cut}$ (see eq. [14] in BMRV), this result leads to the important conclusion that no stable configurations exist for $2GM/Rc^2 > 0.2290$, for large values of $\tilde{T}$. The critical value of central redshift z_c tends likewise to a limiting value corresponding to $(z_c)_{\rm crit} = 0.4832$, for decreasing values of α. The results, using the three different methods, are in complete agreement.

5. LIMITING CASE FOR LOW-TEMPERATURE CONFIGURATIONS WITH HIGH CENTRAL REDSHIFTS

The stability of models with $\alpha < 1.5$ can be approximately estimated from the behavior of the curves $M_\alpha(\rho_c)$. For larger α up to the limiting value, the curve $M_\alpha(\rho_c)$ shows a behavior consisting of one or more loops and in some cases of a curve coming out from the origin. In this case the maximum of $M_\alpha(\rho_c)$ is not good for the investigation of the stability, and it is very difficult to use other methods mentioned in § 1.

The criteria mentioned in § 3 cannot be applied in this regime except for the one based on sequences with constant W_0. This criterion permits us to extend the stability analysis to configurations with $\tilde{T} \lesssim 0.1$ and $z_c \gtrsim 1$.

In order to better analyze the stability of the configurations in such a region we calculated the first maximum of the fractional binding energy E_b/N, with $E_b = (mN - M)c^2$, in the sequences with constant W_0. This procedure is equivalent to that based on the calculation of the maximum mass, especially in the region at small z_c and $\tilde{T} \gtrsim 0.1$, where the total number N is constant near the maximum of the mass M and the results coincide. In the region $\tilde{T} \lesssim 0.1$ and $1 \lesssim z_c \lesssim 4$ the results are slightly different as a result of small variations of the total number N near the maximum of the mass M.

In the isothermal limit of large z_c (or ρ_c) and small enough $\tilde{T}$, the stability analysis can be approximately connected with the behavior of the fractional binding energy as a function uniquely of $\tilde{T}$. We notice that the fractional binding energy of the system is almost constant along the curves $M_{\tilde{T}}(\rho_c)$ at large enough ρ_c, and we find that the maximum occurs at $\tilde{T}_c \simeq 0.06$ in accordance with a particular solution investigated by Bisnovatyi-Kogan & Zeldovich (1969). This result can be interpreted as a transition from the stable (quasi-Newtonian) configurations at $\tilde{T} < \tilde{T}_c$ to the unstable ones at $\tilde{T} > \tilde{T}_c$.

TABLE 3

NUMERICAL RESULTS OF STABILITY ANALYSIS BASED ON METHOD OF ADIABATIC INVARIANT ($\alpha < 1.5$)

α	$\tilde{T}$	z_c	ρ_c	M	R
1.20......	1.80×10^{-1}	4.700×10^{-1}	4.838×10^{0}	2.73982×10^{-2}	2.680×10^{-1}
			4.870×10^{0}	2.73990×10^{-2}	2.679×10^{-1}
			4.902×10^{0}	2.73994×10^{-2}	2.678×10^{-1}
1.20......	1.81×10^{-1}	4.765×10^{-1}	4.986×10^{0}	2.73804×10^{-2}	2.662×10^{-1}
			5.019×10^{0}	2.73810×10^{-2}	2.661×10^{-1}
			5.052×10^{0}	2.73804×10^{-2}	2.660×10^{-1}
1.20......	1.82×10^{-1}	4.786×10^{-1}	5.032×10^{0}	2.73760×10^{-2}	2.656×10^{-1}
			5.065×10^{0}	2.73758×10^{-2}	2.655×10^{-1}
			5.098×10^{0}	2.73756×10^{-2}	2.654×10^{-1}
0.50......	4.67×10^{-1}	4.765×10^{-1}	3.424×10^{0}	3.17737×10^{-2}	2.893×10^{-1}
			3.447×10^{0}	3.17740×10^{-2}	2.889×10^{-1}
			3.470×10^{0}	3.17740×10^{-2}	2.886×10^{-1}
0.50......	4.68×10^{-1}	4.784×10^{-1}	3.451×10^{0}	3.17739×10^{-2}	2.886×10^{-1}
			3.474×10^{0}	3.17740×10^{-2}	2.883×10^{-1}
			3.497×10^{0}	3.17738×10^{-2}	2.880×10^{-1}
0.50......	4.69×10^{-1}	4.802×10^{-1}	3.479×10^{0}	3.17721×10^{-2}	2.881×10^{-1}
			3.502×10^{0}	3.17720×10^{-2}	2.878×10^{-1}
			3.525×10^{0}	3.17716×10^{-2}	2.875×10^{-1}
0.20......	1.19×10^{0}	4.714×10^{-1}	2.920×10^{0}	3.34390×10^{-2}	3.004×10^{-1}
			2.968×10^{0}	3.34410×10^{-2}	2.993×10^{-1}
			3.017×10^{0}	3.34418×10^{-2}	2.982×10^{-1}
0.20......	1.20×10^{0}	4.758×10^{-1}	2.975×10^{0}	3.34423×10^{-2}	2.991×10^{-1}
			3.024×10^{0}	3.34430×10^{-2}	2.980×10^{-1}
			3.074×10^{0}	3.34425×10^{-2}	2.969×10^{-1}
0.20......	1.21×10^{0}	4.802×10^{-1}	3.032×10^{0}	3.34436×10^{-2}	2.977×10^{-1}
			3.082×10^{0}	3.34430×10^{-2}	2.966×10^{-1}
			3.133×10^{0}	3.34412×10^{-2}	2.955×10^{-1}
0.02......	1.21×10^{1}	4.763×10^{-1}	2.782×10^{0}	3.43966×10^{-2}	3.041×10^{-1}
			2.828×10^{0}	3.43980×10^{-2}	3.029×10^{-1}
			2.875×10^{0}	3.43982×10^{-2}	3.017×10^{-1}
0.02......	1.22×10^{1}	4.800×10^{-1}	2.825×10^{0}	3.43998×10^{-2}	3.030×10^{-1}
			2.872×10^{0}	3.44000×10^{-2}	3.018×10^{-1}
			2.920×10^{0}	3.43991×10^{-2}	3.006×10^{-1}
0.02......	1.23×10^{1}	4.874×10^{-1}	2.917×10^{0}	3.44010×10^{-2}	3.006×10^{-1}
			2.965×10^{0}	3.43990×10^{-2}	2.994×10^{-1}
			3.014×10^{0}	3.43958×10^{-2}	2.982×10^{-1}

NOTE.—The second configuration of each group belongs to the equilibrium sequence and corresponds to a Maxwellian configuration. The first and third configurations correspond to non-Maxwellian configurations for small perturbations of the radius R_0. For each value of α, the configuration coinciding with a local maximum for the mass corresponds to the critical one.

The behavior of the fractional binding energy as a function of the temperature $\tilde{T}$ and the central redshift z_c is summarized in Figure 8. The separation between the regions of stable and unstable configurations is clearly denoted by the two chains of the maxima of the fractional binding energy. At $\tilde{T} \gtrsim 0.1$, we have a horizontal chain which, in accordance with the traditional results, identifies the critical value of the central redshift separating the stable from the unstable models: this value is $z_c \simeq 0.5$. In the region of smaller $\tilde{T}$ we have a vertical chain extending up to infinite values of z_c, less high than the horizontal chain, which identifies a critical value of the temperature: this value is $\tilde{T}_c \simeq 0.06$; models with temperatures lower than $\tilde{T}_c$ are always stable, for every value of the central redshift. In the transition zone, where the vertical chain joins the horizontal one, the behavior of the maxima is uncertain and critically depends on the choice of the sequence of models, which makes the determination of the curve of the onset of instability difficult.

It is important to note how the critical curve obtained by calculating the first maxima of the fractional binding energy from the sequences with constant W_0 reproduces, with surprising accuracy, the behavior of the chain in the three-dimensional figure (see also the dashed curve in Figure 9).

These results are not reproduced if one considers (as in SF) sequences with constant α in order to determine the maxima of the fractional binding energy. In fact, it is clear from Figure 9, showing the sequences with constant α in the z_c-$\tilde{T}$ plane, that the reason that the curve of maximum fractional binding energy in SF turns down toward the origin (see curve C in Fig. 1 of SF) is that it was obtained by looking at the maxima along sequences at constant α, whose particular behavior is no longer so regular in the region of small temperatures, where loops at $\alpha > 1.5$ occur. These maxima are neither actual maxima of the fractional binding energy nor they are relevant for the stability analysis.

Figure 8 shows clearly that the claim of SF "Along *any* sequence in the (T_∞, z_c)-plane the magnitude of E_b/N has a local maximum when the sequence crosses the curve C; C thus represents the locus in the (T_∞, z_c)-plane of maximal fractional binding energy" is not correct. Therefore any conclusion about the stability of the models drawn by using the portion of the curve C turning down toward the origin is wrong because that part of the curve does not represent any particular feature of the binding energy. For instance the Ipser (1980) claim, "One convinces himself that the appropriate sequences generally run upwards in the figure. Assuming that the sufficient condition for stability is valid below curve C, the locus of points of
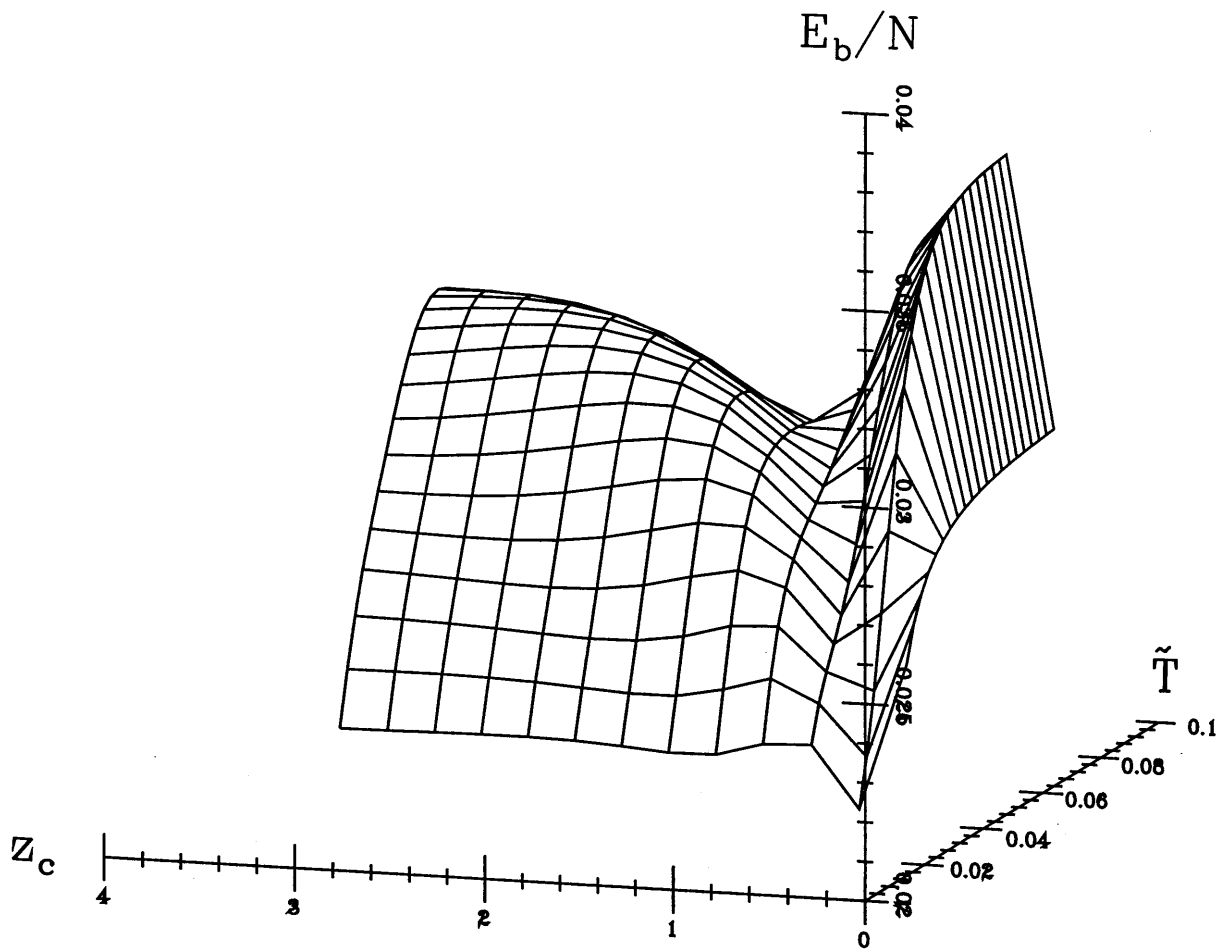
FIG. 8.—Fractional binding energy E_b/N as a function of the central redshift z_c and the temperature $\tilde{T}$

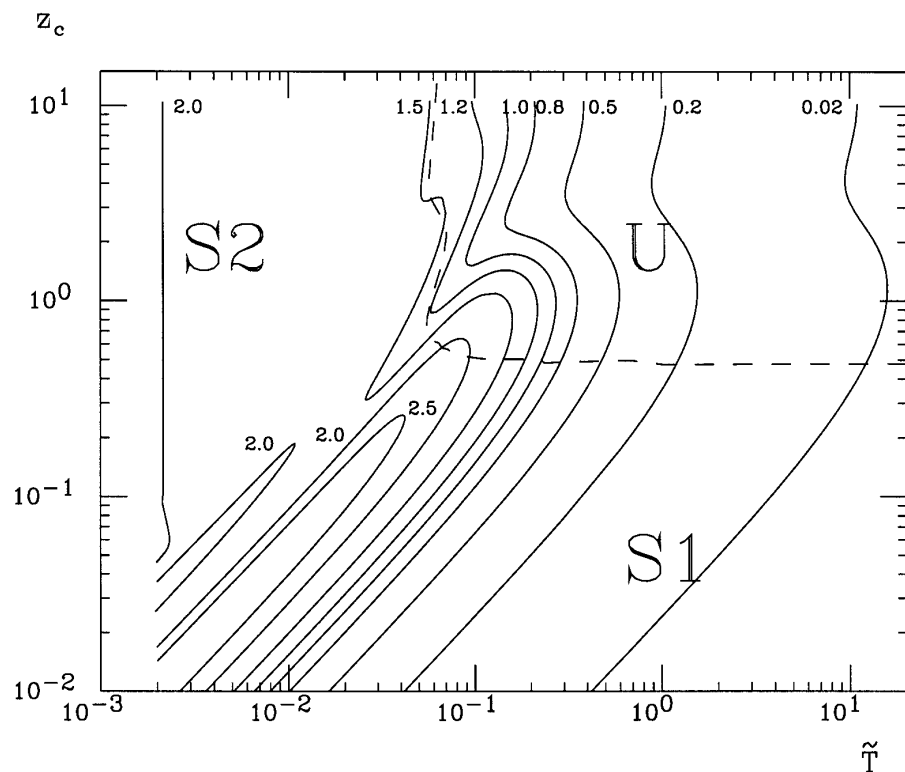FIG. 9.—Sequences at fixed α (labeled on the curves) in the plane z_c-$\tilde{T}$. Dashed line indicates the onset of instability and separates the region U (*unstable models*) from the regions S1 and S2 (*stable models*).

maximum binding energy in the two-dimensional plot, it will follow that the conditions breaks down everywhere along the curve C" must be considered in the light of Figure 8.

6. COMPARISON WITH NUMERICAL MODELS

Rasio, Shapiro, & Teukolsky (1989, hereafter RST) have investigated by numerical simulations the stability of a particular set of equilibrium models up to large values of the central redshift z_c. We would like, for completeness, to recall here some results presented in a letter by Merafina & Ruffini (1995), leading to an explicit relation between the work of RST and ours.

RST adopted a relativistic form of the distribution function f_{RST}, resulting from numerical integrations of the *Newtonian* Fokker-Planck equation for secular evolution of an isotropic stellar cluster during the gravothermal catastrophe. Actually, as it is clear from their Figure 1, the distribution function adopted by RST is slightly different from that used in this paper (eq. [2]) and this leads to some differences in the density profiles, particularly in the size of the configurations.

Even though the functional form of the distribution function adopted by RST is different from the one used in this paper, there is a close relationship between the sequence of models of RST and a particular one of our treatment (Merafina & Ruffini 1995).

The dimensionless energy variable x in the numerical distribution function used by RST is defined as

$$x_{RST} = 13.25\left(\frac{E/mc^2 - 1 + z_c}{z_c}\right), \tag{31}$$

where E is the total energy of a single "particle" defined by equation (4) and z_c is the central redshift of the equilibrium configuration. The range of variation of x_{RST} is determined by the behavior of the total energy E. If we assume that E varies from a minimum value corresponding to a particle at rest in the center of the configuration $E_{min} = mc^2 e^{v_0/2}$ to a maximum given by $E_{max} = mc^2$, the range of variability of x_{RST} is

$$13.25[z_c/(1 + z_c)] \leq x_{RST} \lesssim 13.25 . \tag{32}$$

RST focused their attention on models with $0.123 \leq z_c \leq 3.75$.

In our case, the dimensionless energy variable x used in the distribution function given in equation (2) is

$$x_{BMRV} = E/T , \tag{33}$$

where the minimum energy has the same value given in RST and the maximum energy corresponds to the energy cutoff defined in equation (2). Then the range of variation of x_{BMRV} is

$$\frac{mc^2}{T(1 + z_c)} \leq x_{BMRV} \leq \frac{mc^2}{T} - \frac{\alpha}{2} . \tag{34}$$

If we relate the expression of x_{RST} with that of x_{BMRV} we obtain

$$x_{RST} = 13.25\left(\frac{\tilde{T}x_{BMRV} - 1 + z_c}{z_c}\right), \tag{35}$$

or the inverse expression

$$x_{BMRV} = \frac{z_c}{\tilde{T}}\left(\frac{x_{RST}}{13.25} - 1\right), \tag{35a}$$

where $\tilde{T} = T/mc^2$.

If we consider the same energy range in both treatments, by using equation (34) we obtain the following range of variation of x_{RST}:

$$13.25\left(\frac{z_c}{1 + z_c}\right) \leq x_{RST} \leq 13.25\left(1 - \frac{\alpha\tilde{T}/2}{z_c}\right). \tag{36}$$

In § 3.1 we have defined families of equilibrium configurations with constant central energy cutoff parameter W_0. The relationship that connects the cutoff parameter W_0 with the other relevant parameters characterizing the equilibrium configurations can be obtained by equation (19)

$$\left[W_0 + \frac{\alpha(z_c, \tilde{T})}{2}\right]\tilde{T} = \frac{z_c}{1 + z_c} . \tag{37}$$

If we now turn to identify the configurations considered by RST within our models, we must search for configurations with the same value of the fractional binding energy and the central redshift. The results are given in Table 4 where we have calculated the values of $\tilde{T}$ and W_0 selecting among our models those whose fractional binding energy and central redshift are equal to each of the six configurations investigated by RST (indicated by solid triangles in their Fig. 3). We can conclude from the table that the sequence shown in RST and used by the authors to draw their conclusions about the stability of the models investigated is closely described by a sequence of models with $W_0 \simeq 114$, namely, a particular sequence at constant W_0 among those investigated by our criterion (1). It is clear from Figure 10a the good agreement of the values of $\tilde{T}$ and z_c, given in Table 4, with the analytical relationship indicated in equation (37) for $W_0 = 114$.

TABLE 4

EQUILIBRIUM CONFIGURATIONS WITH THE SAME
REDSHIFT AND FRACTIONAL BINDING
ENERGY OF THE NUMERICAL MODELS
INVESTIGATED BY RST

z_c	$\tilde{T}$	W_0
0.123	9.594×10^{-4}	113.1
0.500	2.881×10^{-3}	114.8
0.750	3.688×10^{-3}	115.0
1.250	4.809×10^{-3}	114.6
2.250	6.027×10^{-3}	113.9
3.750	6.915×10^{-3}	113.2

In Figure 10b we give the behavior of the fractional binding energy E_b/N as a function of the central redshift z_c for the sequence $W_0 = 114$, and we compare these results with the corresponding values in the six models investigated by RST. The accordance is very satisfactory.

It is important to point out that models investigated by RST and found to be stable against relativistic collapse, have $\tilde{T} < \tilde{T}_c$ and thus lie well inside the region of stable configurations of the $z_c - \tilde{T}$ plane. This is confirmed by the existence of a lower limit for W_0 beyond the one all the sequences with constant W_0 are stable: this limit is $W_0 \simeq 15.5$ (see Merafina & Ruffini 1995), while the sequence of models investigated by RST has $W_0 \simeq 114$.

Our analytical results show that there are many families that reach an infinite value of the central redshift without becoming unstable and confirm the results of numerical simulations by RST made on a particular set of solutions.
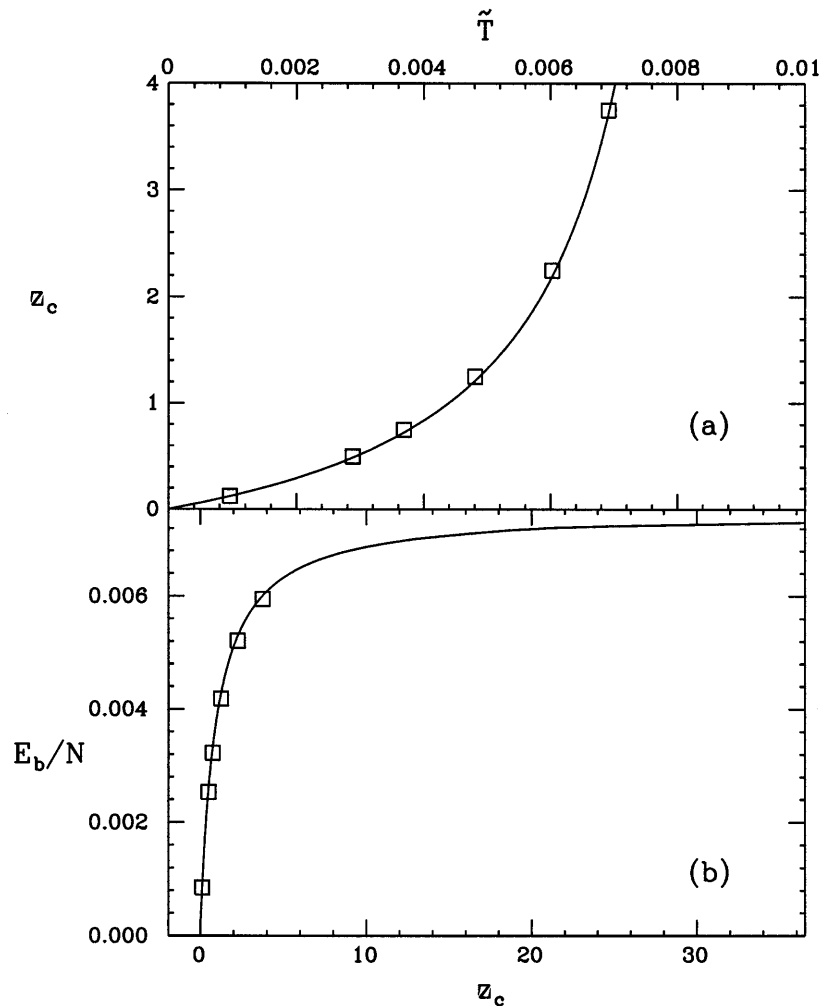

FIG. 10.—(a) Configurations with the same fractional binding energy and central redshift of numerical models investigated by RST (open squares). They fit the analytical function given in eq. (37) for $W_0 = 114$ (continuous line). (b) Numerical model obtained by RST (open squares) and the family of solutions with $W_0 = 114$ (continuous line).

TABLE 5

SUMMARY OF RESULTS OF STABILITY ANALYSIS BY USING DIFFERENT METHODS

	W_0-Constant Sequence	S-Constant Sequence	Adiabatic Invariant Conservation	Fractional Binding Energy
$\tilde{T} > 0.06$:				
$\alpha = 1.20$	$\tilde{T}_{cr} = 0.185$ $z_{c,cr} = 0.496$	$\tilde{T}_{cr} = 0.181$ $z_{c,cr} = 0.474$	$\tilde{T}_{cr} = 0.181$ $z_{c,cr} = 0.477$	
$\alpha = 0.50$	$\tilde{T}_{cr} = 0.473$ $z_{c,cr} = 0.488$	$\tilde{T}_{cr} = 0.468$ $z_{c,cr} = 0.478$	$\tilde{T}_{cr} = 0.468$ $z_{c,cr} = 0.478$	
$\alpha = 0.20$	$\tilde{T}_{cr} = 1.21$ $z_{c,cr} = 0.485$	$\tilde{T}_{cr} = 1.20$ $z_{c,cr} = 0.481$	$\tilde{T}_{cr} = 1.20$ $z_{c,cr} = 0.476$	
$\alpha = 0.02$	$\tilde{T}_{cr} = 12.2$ $z_{c,cr} = 0.484$	$\tilde{T}_{cr} = 12.2$ $z_{c,cr} = 0.484$	$\tilde{T}_{cr} = 12.2$ $z_{c,cr} = 0.480$	
$\alpha = 0$	$\tilde{T}_{cr} = \infty$ $z_{c,cr} = 0.483$	$\tilde{T}_{cr} = \infty$ $z_{c,cr} = 0.483$	$\tilde{T}_{cr} = \infty$ $z_{c,cr} = 0.483$	
$\tilde{T} < 0.06$:				
$z_{c,cr} = 0.994$				$\tilde{T}_{cr} = 0.058$
$z_{c,cr} = 2.191$				$\tilde{T}_{cr} = 0.071$
$z_{c,cr} = 3.040$				$\tilde{T}_{cr} = 0.061$
$z_{c,cr} = 4.216$				$\tilde{T}_{cr} = 0.057$
$z_{c,cr} = \infty$				$\tilde{T}_{cr} = 0.060$

7. CONCLUSIONS

In this paper we have investigated the stability against relativistic collapse of families of equilibrium configurations with different cutoff parameters. The main results can be summarized dividing the z_c-$\tilde{T}$ plane (Fig. 9) into three regions: S1, S2, and U.

1. *S1 − U ($\tilde{T} > 0.06$)*.—These regions of the plane z_c-$\tilde{T}$ correspond to the traditional families of equilibrium configurations whose stability was largely investigated in the past. S1 indicates the part of the plane corresponding to stable equilibria, while U indicates the unstable ones. The three different methods introduced in BMRV give results in agreement among them (see Table 5) and with the results of previous analysis (see, e.g., Ipser 1969 and SF). For large values of the temperature $\tilde{T}$ the critical value of central redshift tends to $(z_c)_{crit} = 0.4832$. In this regime there are not stable configurations with z_c larger than 0.5. Our results confirm this conclusion and are obtained with more accuracy.

2. *S2 ($\tilde{T} < 0.06$)*.—This region of the plane corresponds to extreme core-halo configurations whose stability analysis carried out by SF did not supply conclusive results. In contrast to the conclusions of SF, our results show that these configurations are also stable (see Table 5). As pointed out by Merafina & Ruffini (1997), the dense core is in gravitational equilibrium with a Newtonian envelope, which permits to the system to be stable as a whole.

In order to investigate the stability of these equilibria we have used a binding energy criterion supplying results in good agreement with the ones based on sequences at constant W_0. The other two methods introduced in BMRV do not give results of simple interpretation.

Thus we come to the interesting conclusion that *there exist stable nonsingular configurations with arbitrarily large central redshift*.

It must be noted that the Ipser (1969) and Fackerell (1970) results, also reported in SF, already indicated that models with small temperatures could be stable even for values of the central redshift larger than 0.5 but only until a limiting value of z_c. Nevertheless the authors came to a different conclusion by considering the behavior of the curve of the maxima of the fractional binding energy. Application of these criteria for the particular solution obtained by Bisnovatyi-Kogan & Zeldovich (1969) has shown that it satisfies necessary condition of stability but was unable to establish the sufficient condition (Bisnovatyi-Kogan & Thorne 1970).

We have shown that the curve indicating the onset of instability, obtained by SF, gives correct results only in the region with $\tilde{T} \gtrsim 0.1$, while it represents only the locus of the relative maxima of the fractional binding energy for smaller $\tilde{T}$ and therefore in no way it is related with the analysis of the stability of those equilibrium configurations. Actually it is evident from Figure 8, where the fractional binding energy has been plotted as a function of z_c and $\tilde{T}$, the chain corresponding to the curve separating the region S1 from U and the chain at a lower height corresponding to the curve separating the region S2 from U. The plot shows that the conclusions of SF about the role of the curve C in the stability analysis are not valid.

Finally, we have compared and contrasted the models investigated by RST with our families of configurations with constant W_0. We found that the models of RST correspond to a particular sequence of stable solutions ($W_0 = 114$) belonging to a more general family of stable configurations which can reach arbitrarily large values of z_c.

REFERENCES

Bisnovatyi-Kogan, G. S., Merafina, M., Ruffini, R., & Vesperini, E. 1993, ApJ, 414, 187 (BMRV)
Bisnovatyi-Kogan, G. S., & Thorne, K. S. 1970, ApJ, 160, 875
Bisnovatyi-Kogan, G. S., & Zeldovich, Y. B. 1969, Astrofizika, 5(2), 223, (transl. Astrophysics, 5, 105 [1969])
Chandrasekhar, S. 1939, An Introduction to the Study of Stellar Structure (Chicago: Univ. of Chicago Press)
Einstein, A. 1939, Ann. Math., 40, 922
Fackerell, E. D. 1970, ApJ, 160, 859
Harrison, B. K., Thorne, K. S., Wakano, M., & Wheeler, J. A. 1965, Gravitational Equilibrium and Gravitational Collapse (Chicago: Univ. Chicago Press)
Hoyle, F., & Fowler, W. A. 1967, Nature, 213, 373
Ipser, J. R. 1969, ApJ, 158, 17

Ipser, J. R. 1980, ApJ, 238, 1101
Merafina, M., Bisnovatyi-Kogan, G. S., Ruffini, R., & Vesperini E. 1996, in Proc. 7th M. Grossman Meeting on General Relativity. ed. R. T. Jantzen, & G. MacKeiser (Singapore: World Scientific), A447
Merafina, M., & Ruffini, R. 1989, A&A, 221, 4
———. 1990, A&A, 227, 415
———. 1995, ApJ, 454, L89
———. 1997, Int. J. Mod. Phys. D, in press
Podurets, M. A. 1969, AZh, 46, 126 (transl. Soviet Astron.—AJ, 13, 94 [1969])

Rasio, F. A., Shapiro, S. L., & Teukolsky, S. A. 1989, ApJ, 336, L63 (RST)
Rees, M. J. 1984, ARA&A, 22, 471
Suffern, K. G., & Fackerell, E. D. 1976, ApJ, 203, 477 (SF)
Tolman, R. C. 1939, Phys. Rev. Lett., 55, 341
Zapolsky, H. S. 1968, ApJ, 153, L163
Zeldovich, Y. B. 1963, Voprosy Kosmogonii, 9, 157, (in Russian)
Zeldovich, Y. B., & Podurets, M. A. 1965, AZh, 42, 963 (transl. Soviet Astron.—AJ, 9, 742 [1966]) (ZP)